Frequency-Dependent Electrical Mixing Law Behavior in Spherical Particle Composites

M.A. CAMPO,[1] L.Y. WOO,[1] T.O. MASON[1,*] & E.J. GARBOCZI[2]

[1]*Department of Materials Science and Engineering, Northwestern University, Evanston, IL 60208, USA*
[2]*National Institute of Standards and Technology, Building Materials Division, Gaithersburg, MD 20899, USA*

Abstract. The electrical properties of cement-based composites with mono-size conductive (steel) or insulating (glass) spherical inclusions were investigated by combined 2-point impedance spectroscopy and 4-point dc resistance measurements. The matrix was ordinary Portland cement (w/c = 0.4; cured for 7 days). Particle loading was varied over an extended range to as high as 42% volume fraction. The steel particle composites behaved like the glass particle composites at dc and low ac frequencies; conductivity decreased with increasing particle loading. Under ac excitation, however, the steel particles were rendered conductive; conductivity increased dramatically with particle loading. The results were analyzed in terms of various mixing laws and effective media theories and the proposed "frequency-switchable coating model," which accounts for the unusual frequency-dependent behavior of the steel particle composites.

Keywords: composites, cement, impedance, electrical conductivity, mixing laws

1. Introduction

Recent work has shown that impedance spectroscopy is a useful tool for characterizing the electrical properties of composites [1–7]. This is especially true when certain conditions are met, i.e., the matrix is moderately conductive, the second phase particles or fibers are highly conductive, and a thin, but resistive interfacial "coating" surrounds the particles/fibers within the matrix phase. This layer can be a passive oxide film (e.g., steel particles/fibers in cement-based matrices), an electrochemical double layer/charge transfer resistance (e.g., carbon particles/fibers in cement-based matrices), or a Schottky barrier (e.g., SiC whiskers in Si_3N_4). The result is that the particles/fibers behave as insulating inclusions at dc and low ac frequencies. With increasing frequency, however, displacement currents through the coating short it out, and the particles/fibers now behave as conductive inclusions. A conceptual "frequency-switchable coating model" was developed to describe this behavior [6].

The characteristic feature in impedance spectra of composites with discontinuous conductive (but coated) particles/fibers is the subdivision of a single bulk arc without particles/fibers into two separate arcs with the particles/fibers present, as in Fig. 1. The Nyquist plots (negative imaginary vs. real impedance) shown are for plain ordinary Portland cement paste (OPC) and OPC with a volume fraction of 15% steel or glass ball bearings. Details of their preparation and measurement are given below. Frequency increases from right to left in each plot. To the right of 1640 Ω for the OPC paste and ≈2000 Ω for the two composites is the beginning of a large low frequency electrode arc (due to the embedded steel electrodes in each case). There is only a single bulk arc for the plain OPC (to the left of 1640 Ω) and for the glass ball/OPC composite, albeit shifted to higher resistance (to the left of 2000 Ω). For the steel ball/OPC composite, however, the bulk response (to the left of ≈2000 Ω) consists of two arcs, with an intersection at ≈1000 Ω. We will refer to the frequency and real resistance at this intersection as the "cusp frequency" and cusp resistance (R_{cusp}). The appearance of two arcs is as expected for

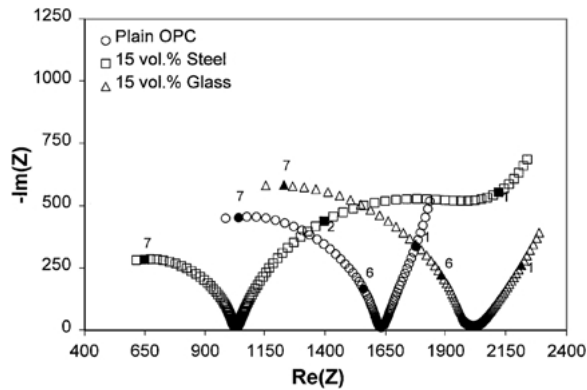*To whom all correspondence should be addressed.

Fig. 1. Typical Nyquist plots for 7 day 15% volume fraction steel and glass ball bearing/OPC composites and plain OPC. The numbers corresponding to darkened points indicate the logarithm (base 10) of the frequency (Hz) values. The minimum value of $-\text{Im}(Z)$ for the steel, plain, and glass samples occurs at a frequency (Hz) value of approximately 10^4.

a conducting sphere coated with an insulating layer [1] and is consistent with the frequency-switchable coating model.

The present work describes experiments involving spherical inclusions, both insulating and conductive, in cement paste as a model system. Cement paste has a moderate ionic conductivity, is easy to process, and readily forms the requisite high resistivity passive oxide film on steel particles due to its intrinsically high pH pore solution [8]. Furthermore, the oxide film should prevent the onset of percolation regardless of particle loading. Finally, the ability to switch the resistance of the coating on (at dc) or off (at the cusp frequency) allows us to investigate electrical mixing law behavior for both insulating and conductive particles. Experiments were also carried out with insulating glass spheres to compare with the dc result for the "coated" steel spheres. A single sphere size was employed in each case. Experiments with distributions of particle sizes will be reported separately.

2. Experimental Procedure

Composites with spherical inclusions, steel ball bearings or glass beads, were prepared from type I ordinary Portland cement (OPC) with a water-to-cement ratio of 0.4 by weight. The dry powder and water were mixed by hand for approximately 3 min prior to blending at high speed in a commercial blender for 2 min to
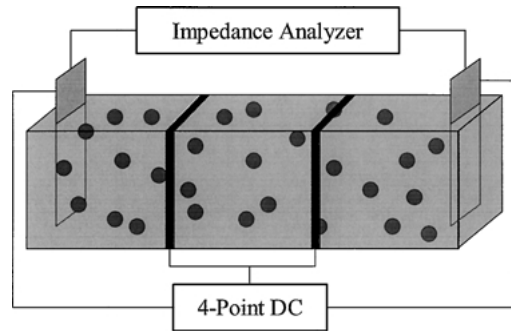

Fig. 2. Experimental set-up for impedance and 4-point dc resistance measurements.

achieve homogeneity. The slurries were allowed to set for an appropriate time (≈ 3 h) to achieve a viscosity sufficient to prevent subsequent settling by the steel ball bearings (3.18 mm diameter, Bearing Distributors, Wheeling, IL) or glass beads (3.0 mm diameter, Fox Industries, Fairfield, NJ), which were mixed in by hand.[1] The viscous mixtures were then cast into rectangular polycarbonate molds (25 mm × 25 mm × 100 mm), as in Fig. 2.

Stainless steel electrodes (20 mm × 30 mm × 0.5 mm) were cast in place 5 mm from each end, yielding an inter-electrode spacing of 90 mm. These embedded electrodes served as 2-point ac impedance electrodes, as well as the outer current electrodes for dc measurements. Samples were stored at 100% RH; they were removed from the molds after 24 h, and impedance measurements were made at seven days. Voltage contacts for 4-point dc measurements were made by tightly wrapping 0.25 mm diameter steel wire loops around the samples, as shown in Fig. 2. Silver paste was painted over the wire loops in 2 mm wide strips to ensure electrical contact with the specimens. An enamel sealant was then used to seal the silver paste to prevent water (and contact) loss at these electrodes.

For 2-point impedance measurements, a Solartron 1260 impedance/gain-phase analyzer was employed with Z-60 personal computer software for data acquisition (Schlumberger, Houston, TX).[1] The excitation voltage was 1 V and scans were performed from 11 MHz to 5 Hz, with data collected at 20 steps per frequency decade. The 4-point dc resistance measurements were carried out with a programmable current source and digital multimeter using LabVIEW[1] personal computer software for data acquisition (Keithley, Models 220 and 2000, Cleveland, OH).[1]

For resistance measurements, current was applied to the outer electrodes of Fig. 2 in increments of 1 mA from 10 mA to −10 mA. In certain instances current was increased to ±50 mA. The voltage drop between the center electrodes was recorded at each current level. Specimen resistance was calculated from the slope at the origin in current vs. voltage plots.

3.   Results and Discussion

Typical impedance results for a 7 day old 20% volume fraction steel ball bearing/OPC composite are compared to the results for a plain OPC specimen of identical age in Fig. 3. In each case, the value of R_{DC} value is that obtained from 4-point dc measurements, corrected for the longer inter-electrode spacing of the 2-point vs. the 4-point geometries. There is good agreement between R_{DC} and the impedance intersection at ≈1700 Ω between the single bulk arc and the electrode arc for the plain OPC sample. Similarly, the value of R_{DC} for the composite is consistent with the impedance cusp at ≈2250 Ω between the bulk features (to the left) and the electrode arc (to the right). It should be pointed out that there is often strong convolution between the rightmost bulk arc and the electrode arc, as exhibited here and in Fig. 4(b) (described below). This can prevent an accurate evaluation of the dc resistance, based upon impedance measurements alone. For conductive particle/fiber composites, it is
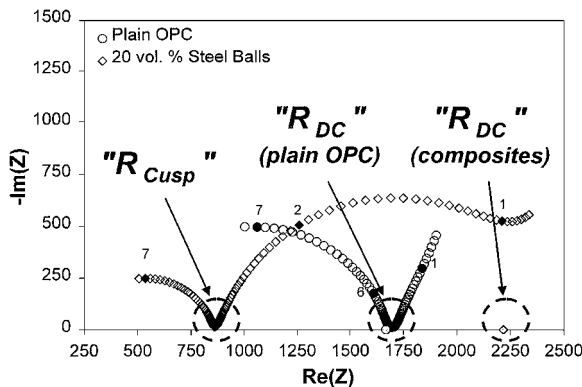

Fig. 3. Typical Nyquist plots for a 7 day 20% volume fraction steel ball bearing/OPC composite and plain OPC with R_{cusp} and R_{DC} labeled. The numbers corresponding to darkened points indicate log frequency (Hz) values. The minimum −Im(Z) for the steel and plain samples occurs at a log frequency (Hz) value of ≈4.
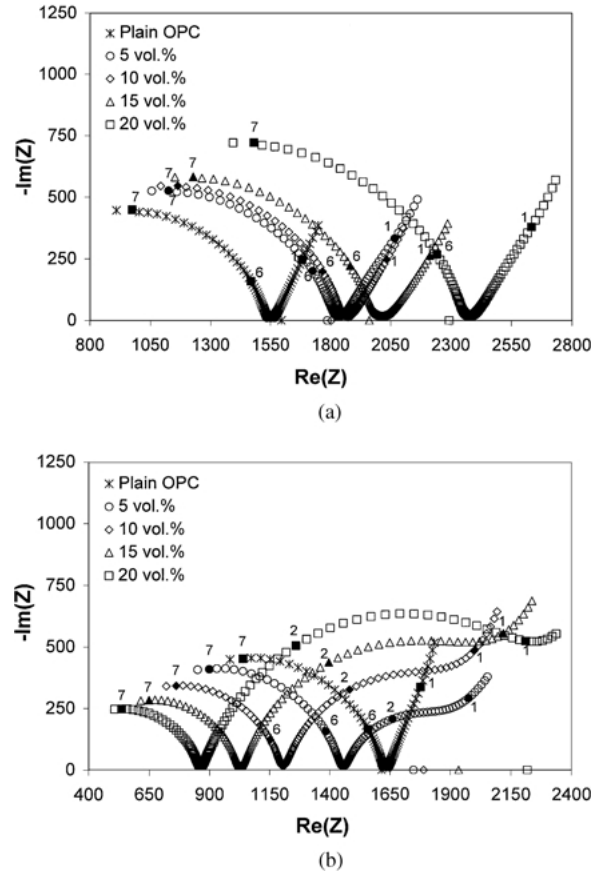

Fig. 4. Trends by volume fraction of (a) glass ball bearing/OPC composites and (b) steel ball bearing/OPC composites. Four-point dc values are shown for comparison on the Re(Z) axis. The numbers corresponding to darkened points indicate log frequency (Hz) values. The minimum −Im(Z) for the samples occurs at a log frequency (Hz) value of ≈4.

therefore advisable to make independent 4-point dc resistance measurements, as was done in the present work.

Figure 4(a) and (b) display impedance spectra for plain OPC and composites at 5% volume fraction increments up to 20% for insulating (glass) and conductive (steel) ball composites, respectively. As illustrated in Fig. 1, the addition of glass beads does not significantly alter the shape of the impedance spectra, but shifts them progressively along the real impedance axis in Fig. 4(a) (increasing resistivity). Also shown are the dc resistances, which agree well with the bulk-electrode cusp values in the impedance spectra to within an estimated ±10% uncertainty. This is based upon an approximate 5% uncertainty in inter-electrode spacing in
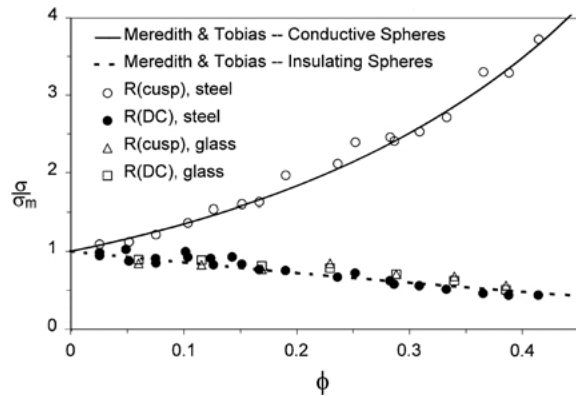
Fig. 5. Normalized conductivity of steel and glass ball bearing/OPC composites plotted with Meredith and Tobias formulas.

Fig. 6. Conceptual model for the current flow (a) at dc and (b) at the cusp frequency under ac excitation.

each experiment and is consistent with experimental reproducibility.

With the addition of steel ball bearings, the spectra of Fig. 4(b) consistently show the dual-arc bulk response of Fig. 1, as described above. The bulk-electrode cusp point, when clearly observed, is consistent with the 4-point dc resistance value, and increases monotonically with the volume fraction of ball bearings. At the same time, the bulk cusp resistance (between the two bulk arcs) decreases monotonically with increasing volume fraction of ball bearings.

Figure 5 displays normalized conductivity values, σ(composite)/σ(matrix), vs. volume fraction of particles (steel or glass balls) in 7 day samples. The upper line in Fig. 5 is derived from the cusp resistance (the intersection of the two bulk arcs) for the steel ball bearing composites, with the matrix value coming from the dc resistance of OPC paste. There are three sets of data on the lower line. Two of them are for glass bead composites, one employing the bulk-electrode cusp value from the impedance plots vs. R_{DC} for OPC paste and the other using R_{DC} values exclusively. There is good agreement between the two approaches. The third set of data is the value of R_{DC} from 4-point dc measurements for steel ball composites. Of great interest is the fact of the agreement between the dc resistance values of the steel and glass ball composites. The model lines in the two cases will be discussed further below.

The behavior in Fig. 5 provides confirmation of the freqency-switchable coating model [6]. Figure 6 shows a conceptual model for current flow at dc (Fig. 6(a)) vs. that at the cusp frequency under ac excitation (Fig. 6(b)). The highly resistive oxide film surrounding
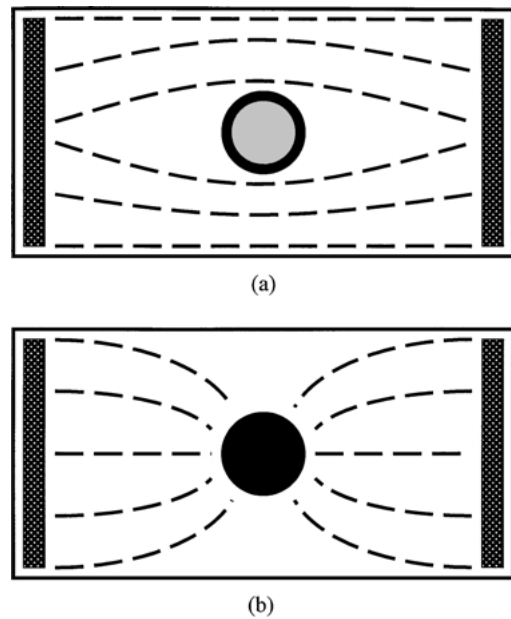
a steel ball bearing electrically isolates it from the matrix at dc and low ac frequencies, and the ball behaves as if it were an insulating sphere. The balls not only reduce the volume fraction of matrix (the conducting phase) but cause current to be constricted to regions between particles. Hence, resistance increases (Fig. 4(b)) and conductivity decreases (Fig. 5). At the cusp frequency, however, displacement currents have shorted out the oxide film, and the ball becomes a short-circuit path for current flow through the matrix. Composite resistance decreases (Fig. 4(b)) and conductivity increases dramatically (Fig. 5).

The absence of a percolation threshold, even for the conductive sphere composites under ac excitation, requires comment. Due to the oxide film, we do not anticipate a dc percolation threshold under fields up to the breakdown strength of the oxide film surrounding the particles. However, the oxide film resistance is no longer in effect at the cusp frequency in the ac experiments. The absence of an ac percolation threshold with loading levels up to 42% volume fraction of steel ball bearings is noteworthy. The reason for this may be that cement particles (median particle size $\approx$10 μm) completely coat the balls during processing. At closest approach, adjacent particles will be separated by at least 10 μm. Later, hydration products replace the

parent cement particles in the inter-particle space. For this reason, the steel particle/OPC system provides a unique opportunity to study mixing law behavior for the electrical properties of such composites, without the onset of percolation.

There have been several outstanding reviews of mixing laws and effective media theories for electrocomposites [9–12]. In the dilute limit, all such equations should reduce to Maxwell's equation:

$$\frac{\sigma}{\sigma_m} = 1 + \left[\frac{3(\Delta - 1)}{(\Delta + 2)}\right]\phi + 0\,(\phi^2) \qquad (1)$$

where σ is the conductivity of the composite, σ_m is the conductivity of the matrix phase, Δ is the ratio of particle conductivity to that of the matrix, ϕ is the volume fraction of particles, and higher-order terms are neglected. In the case of conducting spheres, $\Delta = \infty$ and the first-order coefficient, otherwise known as the "intrinsic conductivity" [13], is 3. With insulating spheres ($\Delta = 0$) the intrinsic conductivity is $-3/2$.

Other models extend calculations beyond the dilute range. The Maxwell-Wagner equation (also known as the Maxwell-Garnett equation [12] or Wiener's rule [11]) based on the well-known Clausius-Mossoti equation, is given by [11]:

$$\left(\frac{\sigma - \sigma_m}{\sigma + 2\sigma_m}\right) = \left(\frac{\sigma_p - \sigma_m}{\sigma_p + 2\sigma_m}\right)\phi \qquad (2)$$

where σ_p is the particle conductivity. This model is formally equivalent to the Hashin-Shtrikman lower bound (conductive particles) and upper bound (insulating particles) [11, 14] and will be referred to as the "MW-HS" equation(s).

Bruggeman's asymmetric (BA) medium theory [11] for conducting spheres is given by:

$$\frac{\sigma}{\sigma_m} = (1 - \phi)^{-3} \qquad (3)$$

wheras for insulating spheres the BA equation is:

$$\frac{\sigma}{\sigma_m} = (1 - \phi)^{3/2} \qquad (4)$$

Zuzovsky and Brenner performed calculations for the effective conductivity of a simple cubic array of spheres embedded in a matrix vs. volume fraction of spheres [15]:

$$\frac{\sigma}{\sigma_m} = 1 - 3\phi\left[\left(\frac{2 + \Delta}{1 - \Delta}\right) + \phi - \frac{1.306\phi^{10/3}}{\frac{(\frac{4}{3} + \Delta)}{(1 - \Delta)} + 0.4072\phi^{7/3}}\right.$$
$$\left. - \frac{2.218 \times 10^{-2}(1 - \Delta)\phi^{14/3}}{(\frac{6}{5} + \Delta)} + 0\,(\phi^6)\right]$$
$$(5)$$

Finally, Meredith and Tobias [10] extended Fricke's treatment [16] of ellipsoidal particles within a Clausius-Mosotti framework by mixing half of the spheres at a given volume fraction, calculating the composite conductivity, and using this as the matrix for a new composite made with the addition of the other half of the spheres. The resulting equations are:

$$\frac{\sigma}{\sigma_m} = \frac{(1 + \phi)(2 + \phi)}{(1 - \phi)(2 - \phi)} \qquad (6)$$

for conducting spheres and

$$\frac{\sigma}{\sigma_m} = \frac{8(2 - \phi)(1 - \phi)}{(4 + \phi)(4 - \phi)} \qquad (7)$$

for insulating spheres.

The various mixing laws and effective media theories are plotted vs. particle volume fraction in Fig. 7 for the case of conductive spheres, with the experimental data of the present study superimposed. The Meredith-Tobias equation exhibits the best agreement
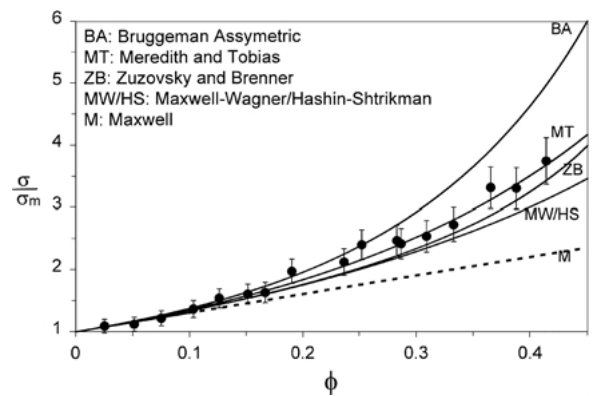

Fig. 7. Various mixing laws and effective media theories plotted vs. particle volume fraction for conductive spheres, with the experimental data superimposed.

with the experimental results. The Zuzovsky-Brenner model comes close; however, this model is for an ordered array of particles, which is clearly not the case in the present work. The Bruggeman asymmetric medium equation exhibits a markedly higher conductivity. This is not unexpected, since the BA model is most applicable for a wide range of particle sizes as opposed to the single size in the present work. As expected, all the models approach the Maxwell line for volume fractions less than 0.1, the oft-quoted upper limit for the dilute regime. The slope of 3 in this regime is exactly the intrinsic conductivity of conducting spheres [13].

The Meredith-Tobias equation can be factored to determine the higher-order coefficients in the virial expansion of Eq. (1). The resulting equation is:

$$\frac{\sigma}{\sigma_m} = 1 + 3\phi + \sum_{n=2}^{\infty}\left(3 + \sum_{m=2}^{n}\frac{1.5}{2^{m-2}}\right)\phi^n \quad (8)$$

and the first few terms are given in Table 1. The second-order coefficient is of interest, since this has been independently calculated to be 4.51 [17, 18], in excellent agreement with the value of 4.5 obtained by factoring the Meredith-Tobias equation.

The corresponding plot in the insulating particle regime was inconclusive and has not been shown. There is considerable scatter in the experimental data and the various mixing laws/effective media equations are quite similar. Although we cannot conclusively determine which model is best for the insulating particle regime, it is interesting to note that the Meredith-Tobias model factors to:

$$\frac{\sigma}{\sigma_m} = 1 - \frac{3}{2}\phi + \frac{9}{16}(\phi^2) + 0\,(\phi^3) \quad (9)$$

where the second-order coefficient of 0.5625 is in good agreement with the calculated value of 0.588

Table 1. Values of the coefficients in the factored Meredith-Tobias equation: $\sigma/\sigma_m = 1 + a\phi + b\phi^2 + c\phi^3 + \ldots$.

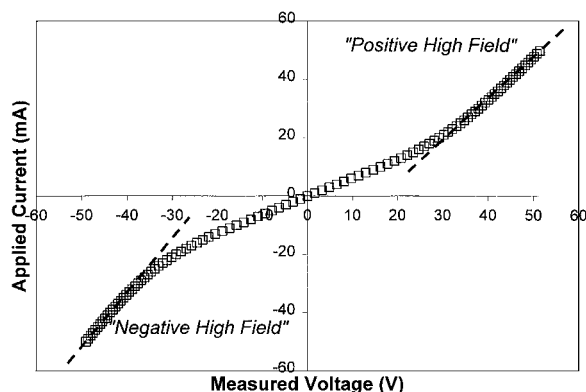| Power of ϕ	Conductive particle coefficients	Insulating particle coefficients
1	$a = 3$	$a = -1.5$
2	$b = 4.5$	$b = +0.5625$
3	$c = 5.25$	$c = -0.09375$
4	$d = 5.625$	$d = +0.03516$
5	$e = 5.8125$	$e = -0.00586$

Fig. 8. Symmetric *I-V* curve where current was applied in pulses from 50 mA to −50 mA, waiting 20 s between each current application.

[17, 18], and higher-order terms are negligibly small (see Table 1). The first-order coefficient of −3/2 is consistent with the known intrinsic conductivity of insulating spheres [13].

In recent work we extended 4-point resistance measurements of steel fiber-reinforced composites to higher current densities [19]. The resulting *I-V* plots looked virtually identical to Fig. 8, which was measured in the present work by increasing applied current to ±50 mA. It was found that the increased slope above the threshold voltage (in the high current or low resistance regime) corresponded to R_{cusp} in the corresponding impedance diagrams. Similarly, the central slope (low current or high resistance regime) agrees with the bulk-electrode intersection in impedance diagrams; R_{DC} is determined from this slope. It was argued that at the threshold voltage, local fields are sufficient to drive interfacial reactions into active or trans-passive corrosion regimes; the oxide film resistance is eliminated. It would seem that steel inclusions can be rendered "conductive" by means of increased frequency (in ac measurements) or by increased field strength (in dc measurements).

There are problems, however, with high-field dc measurements in cement-based composites. First, corrosion products are anticipated on particle surfaces if high dc currents are applied for any period of time [20]. Second, such currents can lead to joule heating effects [21]. The data in Fig. 8 were taken with 20 s delays between individual points to allow for thermal relaxation. If this procedure was not employed, the threshold voltages under negative vs. positive bias differed significantly, and the outer (high

current) regimes had different slopes. Finally, the resistances in the high-current regime were found to be significantly higher than R_{cusp} in impedance measurements. One proposed explanation is that high local current densities (between particles) can result in permanent microstructural changes in the matrix [21]. In contrast, impedance spectroscopy is non-destructive and the only reliable means of assessing composite electrical properties in the "conductive" particle regime.

Conclusions

By combined 4-point dc resistance and 2-point impedance spectroscopy measurements, the electrical properties of cement-based composites with mono-size steel or glass spheres were measured over a wide range of volume fractions (up to 42%). A highly resistive passive oxide film on the steel particles causes the composites to behave like the corresponding glass particle composites. With increasing frequency, however, displacement currents through the oxide films short them out, rendering the particles "conductive" relative to the matrix. This behavior is consistent with the previously proposed "frequency-switchable coating model."

The steel particle-cement matrix system is unique in that no percolation threshold is observed in dc or ac measurements. This is due to the combination of the passive oxide film on the steel particles (no dc percolation, even with immediate contact) and the unavoidable coating of large particles with cement particles during processing. This keeps adjacent particles apart during mixing. Later, hydration products replace the parent cement grains in the inter-particle spaces.

The conductivity vs. volume fraction behavior of spherical particle composites was investigated in both the insulating particle and conductive particle regimes, and compared with various mixing law and effective media theories. The behavior was best described in both regimes by the model of Meredith and Tobias. In the dilute limit, the "intrinsic conductivities" were 3 and $-3/2$ for conducting and insulating spheres, respectively.

High-current 4-point dc resistance measurements were found to yield different conductivities for steel particle composites, as compared to the impedance-derived values. This is thought to be due to permanent changes induced in the matrix phase by the high current densities employed. Therefore, impedance spectroscopy is the only reliable means of measuring conductive particle composite behavior in cement-based matrices.

Acknowledgments

Note

1. Certain commercial equipment is identified in this paper in order to adequately specify the experimental procedure. In no case does such identification imply recommendation or endorsement by the National Institute of Standards and Technology, nor does it imply that the equipment used is necessarily the best available for the purpose.

References

1. R. Gerhardt, *Proc. Cer. Eng. Sci.*, **15**, 1174 (1994).
2. C.A. Wang, Y. Huang, Y. Li, and Z. Zhang, *J. Am. Ceram. Soc.*, **83**, 2689 (2000).
3. J.M. Torrents, T.O. Mason, and E.J. Garboczi, *Cem. Concr. Res.*, **30**, 585 (2000).
4. R.A. Gerhardt and R. Ruh, *J. Am. Ceram. Soc.*, **84**, 2328 (2001).
5. R.A. Gerhardt, J. Runyan, C. Sana, D.S. McLachlan, and R. Ruh, *J. Am. Ceram. Soc.*, **84**, 2335 (2001).
6. J.M. Torrents, T.O. Mason, A. Peled, S.P. Shah, and E.J. Garboczi, *J. Mater. Sci.*, **36**, 4003 (2001).
7. T.O. Mason, M.A. Campo, A.D. Hixson, and L.Y. Woo, *Cem. Concr. Comp.*, **24**, 457 (2002).
8. S.J. Ford, J.D. Shane, and T.O. Mason, *Cem. Concr. Res.*, **28**, 1737 (1998).
9. R. Landauer, in *Electrical Transport and Optical Properties of Inhomogeneous Media*, edited by J.C. Garland and D.B. Tanner, AIP Conf. Proc., Vol. 40 (American Institute of Physics, New York, 1978), p. 2.
10. R.E. Meredith and C.W. Tobias, in *Advances in Electrochemistry and Electrochemical Engineering*, edited by C.W. Tobias, Vol. 2 (Interscience, New York, 1962), p. 15.
11. D.S. McLachlan, M. Blaszkiewicz, and R.E. Newnham, *J. Am. Ceram. Soc.*, **73**, 2187 (1990).
12. C.-W. Nan, *Prog. Mat. Sci.*, **37**, 1 (1993).
13. J.F. Douglas and E.J. Garboczi, in *Advances in Chemical Physics, Vol. XCI*, edited by I. Prigogine and S.A. Rice (John Wiley, 1995), p. 85.
14. Z. Hashin and S. Shtrikman, *J. Appl. Phys.*, **33**, 3125 (1962).

15. M. Zuzovsky and H. Brenner, *J. Appl. Math. Phys.*, **28**, 979 (1977).

16. H. Fricke, *Phys. Rev.*, **24**, 575 (1924).

17. H.B. Levine and D.A. McQuarrie, *J. Chem. Phys.*, **49**, 4181 (1968).

18. D.J. Jeffrey, *Proc. R. Soc. London A*, **335**, 355 (1973).

19. A.D. Hixson, L.Y. Woo, M.A. Campo, and T.O. Mason, *Cem. Concr. Res.*, in press.

20. S.J. Ford and T.O. Mason, in *Mechanisms of Chemical Degradation of Cement-based Systems*, edited by K.L. Scrivener and J.F. Young (E & FN Spon, New York, 1997), p. 126.

21. D. Sohn and T.O. Mason, *Advn. Cem. Bas. Mat.*, **7**, 81 (1998).